

Directional transport of active particles confined in 3D(three dimensional) smooth corrugated channel

Bing Wang, Wenfei Wu

School of Mechanics and Optoelectronics Physics, Anhui University of Science and Technology, Huainan, 232001, P.R.China

E-mail: hnitwb@163.com

Abstract. The transport phenomenon of active particles confined in 3D(three dimensional) corrugated confined channel with Gaussian noises is investigated. Large noise intensity perpendicular to the symmetry axis is good for the diffusion and current along the axis. The generalized resonance transport phenomenon appears with increasing noise intensity parallel to the symmetry axis. Large noise intensity parallel to axis can suppress the diffusion. The diffusion coefficient has a maximum with increasing polar angle noise intensity. There exists an optimal value of parameter f that result in maximum movement speed. Large f is good for the diffusion. Transport reverse phenomenon appears with increasing channel parameter ε and Δ . Too large or too small values of ε and Δ can suppress the diffusion.

Active particles are able to take up energy from environment and convert the energy to directional motion. Investigation of active particles system has enabled to mimic and dissect mechanisms in biological systems[1]. These investigations have grown substantially both in theory and application[2, 3, 4, 5, 6, 7, 8, 9], especially, particles confined in spatial space. There are numerous realizations of confine active particles in nature ranging from bacteria and spermatozoa to artificial colloidal micro-swimmers, e.g., biological cells[10, 11], ion channels[12], nanoporous materials[13, 14], zeolites[15], microfluidic channels[16], artificial nanopores[17], and ionpumps [18].

Confined active particles shows a series of interesting phenomena, e.g. current reversal[19, 20, 21], self-organization[22, 23] and so on. Ghosh *et al.* investigated active overdamped microswimmers in a two-dimensional periodically compartmentalized channel and proved that ratcheting of Janus particles can be orders of magnitude stronger than for ordinary thermal potential ratchets and thus experimentally accessible[24]. Ao *et al.* investigated the transport diffusivity of Janus particles in the absence of external biases with reflecting walls and found the self-diffusion can be controlled by tailoring the compartment geometry[25]. Bechinger *et al.* given an overview of experimental achievements connected to the realization of artificial microswimmers and nanoswimmers[26]. Murali *et al.* showed that geometric constraints are a route to affect the emergent noise properties of a single active particle[27]. Liu *et*

al. investigated the entropic stochastic resonance when a self-propelled Janus particle moves in a double-cavity container[28]. Li *et al.* studied the transport of noninteracting anisotropic particles in a narrow two dimensional left-right and up-down asymmetrical channel[29]. Pototsky *et al.* considered a colony of point like self-propelled surfactant particles without direct interactions that cover a thin liquid layer on a solid support[30].

Previous research considers the particles confined in two dimensions (2D) corrugated channel. In this paper, we investigate the directional transport of active particles confined in a three dimensions(3D) corrugated channel. The paper is structured as follows. Section 1 gives the model considered in this paper. Section 2 analyses the effects of the channel and noise on the system. A concluding discussion is offered in section 3.

1. Basic model and methods

In this work, we consider active particles confined in a 3D smooth corrugated channel with Gaussian white noises. The dynamic of the particle is governed by the following dimensionless equations[31, 32, 33]

$$\frac{\partial x}{\partial t} = v_{0x} + \xi_x(t) = v_0 \sin \theta(t) \cos \varphi(t) + \xi_x(t), \quad (1)$$

$$\frac{\partial y}{\partial t} = v_{0y} + \xi_y(t) = v_0 \sin \theta(t) \sin \varphi(t) + \xi_y(t), \quad (2)$$

$$\frac{\partial z}{\partial t} = v_{0z} + \xi_z(t) = v_0 \cos \theta(t) + \xi_z(t), \quad (3)$$

$$\frac{\partial \theta(t)}{\partial t} = \xi_\theta(t), \quad (4)$$

$$\frac{\partial \varphi(t)}{\partial t} = \xi_\varphi(t). \quad (5)$$

Here, v_0 is the self-propelled speed of the active particle. The polar angle between v_0 and z axis is $\theta(t)$. The azimuth angle between projection of v_0 on xoy plane with x axis is $\varphi(t)$. ξ_x , ξ_y and ξ_z are the noises and parallel to x axis, y axis and z axis, respectively. ξ_θ and ξ_φ are the angle noises, respectively. $\xi_i (i = x, y, z, \theta, \varphi)$ satisfies the following relations.

$$\langle \xi_i(t) \rangle = 0, (i = x, y, z, \theta, \varphi), \quad (6)$$

$$\langle \xi_i(t) \xi_j(s) \rangle = \delta_{ij} Q_i \delta(t - t'), (i = x, y, z, \theta, \varphi), \quad (7)$$

$\langle \dots \rangle$ denotes an ensemble average over the distribution of the random forces. $Q_i (i = x, y, z, \theta, \varphi)$ is the noise intensity. Normally, the noise intensity relates to temperature T . For a charged particle, ξ_i can be effected by the external electric field intensity. As electric field intensity is a vector quantity, so the noise intensity Q_x , Q_y , Q_z , Q_θ and Q_φ can take different value.

Directional transport of active particles confined in 3D (three dimensional) smooth corrugated channel

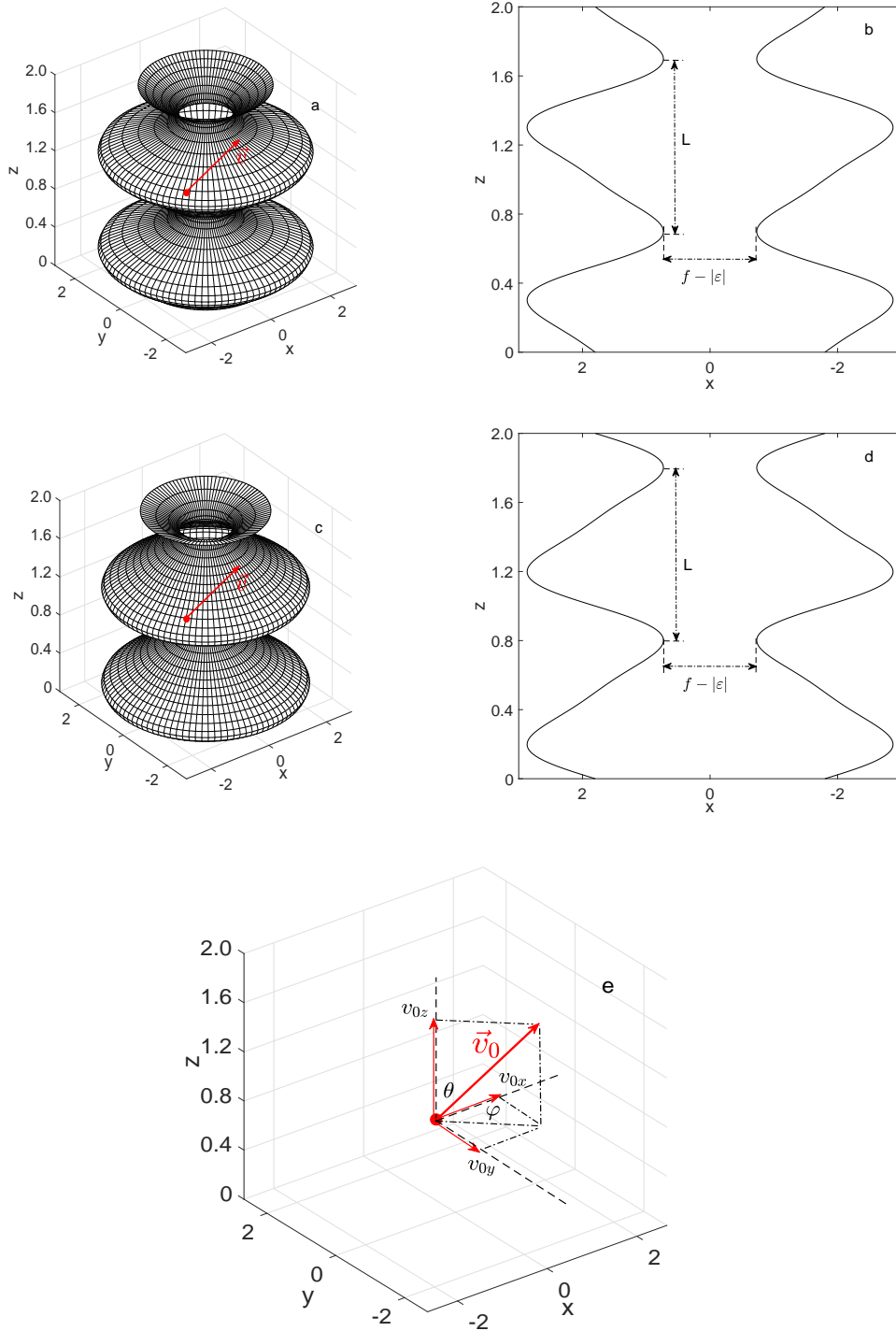


Figure 1. (a) Illustrations of the smooth 3D corrugated channel with $L = 1.0$, $\varepsilon = 1.0$, $f = 1.8$ and $\Delta = -0.8$; (b) Front view of the channel with $L = 1.0$, $\varepsilon = 1.0$, $f = 1.8$ and $\Delta = -0.8$; (c) Illustrations of the smooth 3D corrugated channel with $L = 1.0$, $\varepsilon = 1.0$, $f = 1.8$ and $\Delta = 0.8$; (d) Front view of the channel with $L = 1.0$, $\varepsilon = 1.0$, $f = 1.8$ and $\Delta = 0.8$; (e) The particle with self-propelled velocity \vec{v}_0 confined in the channel.

In this paper, the particles are confined in a 3D smooth corrugated channel. The channel is periodic in space along the z -axis as shown in Fig.1 and is defined by the following sinusoidal function[34]

$$W(z) = \varepsilon[\sin(\frac{2\pi z}{L}) + \frac{\Delta}{4} \sin(\frac{4\pi z}{L})] + f. \quad (8)$$

The shape of the channel are controlled by the parameters ε , f and Δ . In order the channel can not becomes a enclosure space and the particles can transport the channel, the parameter $f > 0$. The diameter of the pore is $f - |\varepsilon|$ (Fig.1) and $f - |\varepsilon| > 0$.

A central practical question in the theory of Brownian motors is the over all long time behavior of the particle, and the key quantities of particle transport is the particle velocity $\langle V \rangle$ and the time-independent diffusion coefficient D [35]. Because particles along the x and y directions are confined, we only calculate the z direction average velocity

$$\langle V \rangle = \lim_{t \rightarrow \infty} \frac{\langle z(t) - z(t_0) \rangle}{t - t_0}, \quad (9)$$

$z(t_0)$ is the position of the particle at time t_0 .

The time-independent normal diffusion coefficient is given by[36]

$$D = \lim_{t \rightarrow \infty} \frac{\langle z^2(t) \rangle - \langle z(t) \rangle^2}{2t}. \quad (10)$$

2. Results and discussion

In this letter, we demonstrate the transport phenomenon of active particles confined in a 3D smooth corrugated channel. In order to give a clear analysis of the system. Eqs.(1, 2, 3, 4, 5) are integrated using the Euler algorithm. The integration step time $\Delta t = 10^{-4}$ and the total integration time is more than 10^5 . The stochastic averages are obtained as ensemble averages over 10^5 trajectories.

The average velocity $\langle V \rangle$ and diffusion coefficient D as functions of x axis noise intensity Q_x is reported in Fig.2. In Fig.2(a), $\langle V \rangle > 0$ when x axis noise does not exist($Q_x = 0$). $\langle V \rangle < 0$ when $Q_x \neq 0$, so the particle moves in $-z$ direction when x axis noise exist. The average speed $|\langle V \rangle|$ increases with increasing Q_x , and the slope of $\langle V \rangle - Q_x$ curve decreases with increasing Q_x and changes to zero when Q_x is large. So small x axis noise intensity will inhibit current in $-z$ direction, and large x axis noise intensity is good for this current. The effect will become weak when x axis noise intensity is too large. In Fig.2(b), the diffusion coefficient D increases with increasing Q_x , so large x axis noise is good for the diffusion. In Fig.2(c), the average velocity $\langle V \rangle$ ($\langle V \rangle > 0$) increases with increasing Q_x . The slope of $\langle V \rangle - Q_x$ curve decreases with increasing Q_x and changes to zero when Q_x is large. So large x axis noise intensity is good for the current in $+z$ direction. In Fig.2(d), just like the result of Fig.2(b), D increases with increasing Q_x , namely large x axis noise is good for the diffusion too.

The average velocity $\langle V \rangle$ and diffusion coefficient D as functions of y axis noise intensity Q_y is reported in Fig.3. Just like the effect of x axis noise(Fig.2), when

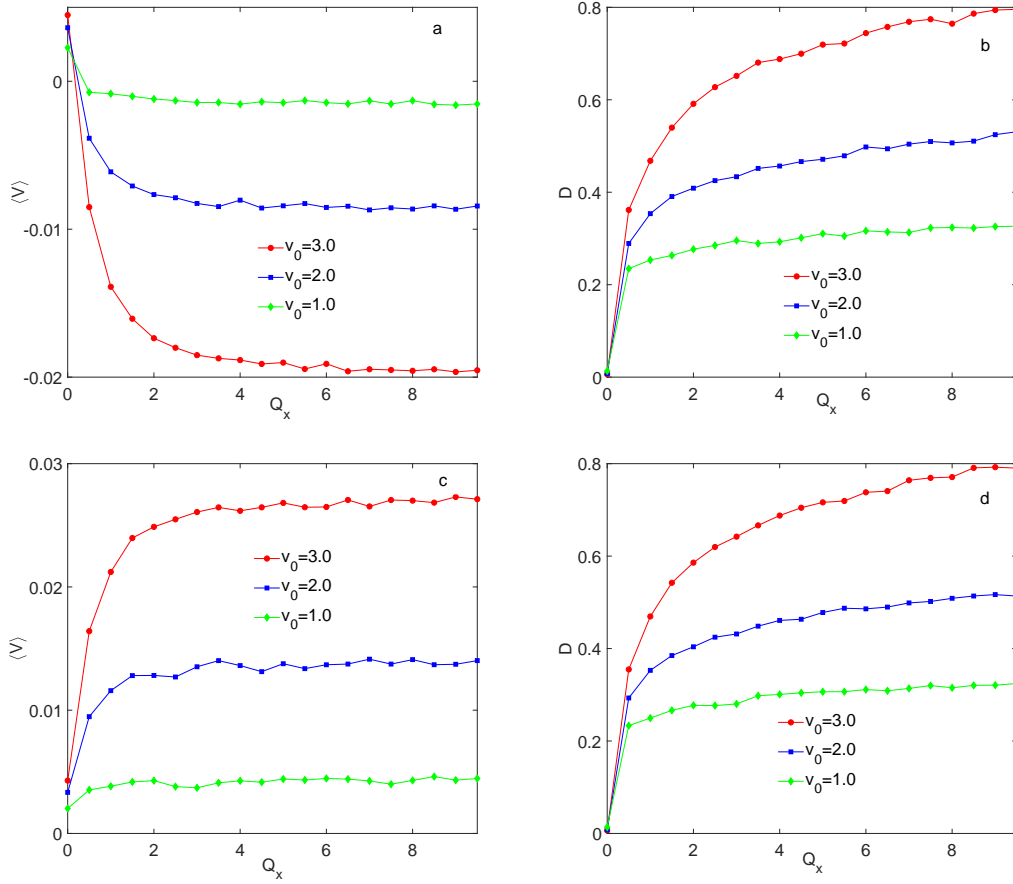


Figure 2. The average velocity $\langle V \rangle$ and diffusion coefficient D as functions of Q_x for different self-propelled speed v_0 . The other parameters are $L = 1.0$, $\varepsilon = 1.0$, $f = 1.8$, $Q_y = Q_z = 1.0$, $Q_\theta = Q_\varphi = 0.5$: (a) $\Delta = -0.8$, (b) $\Delta = -0.8$, (c) $\Delta = 0.8$, (d) $\Delta = 0.8$.

$\Delta = -0.8$ (Fig.3(a) and Fig.3(b)), $\langle V \rangle > 0$ when $Q_y = 0$. When $Q_y \neq 0$, the particle moves in $-z$ direction. The average speed $|\langle V \rangle|$ and diffusion coefficient D monotonic increases with increasing Q_y . $\langle V \rangle - Q_y$ and $D - Q_y$ curves change to horizon when Q_y is large. When $\Delta = 0.8$ (Fig.3(c) and Fig.3(d)), the particle moves in $+z$ direction. $|\langle V \rangle|$ and D monotonic increase with increasing Q_y . The $\langle V \rangle - Q_y$ and $D - Q_y$ curves change to horizon when Q_y is large. So large y axis noise intensity is good for diffusion and the current in $-z$ and $+z$ direction, but the effects will become weak when the noise intensity is large. From Figs.2 and 3, we find x axis noise and y axis noise have the same effect on the system. This is because the channel is axis-symmetric, so x axis and y axis noises are equivalent for the system. In Figs.2 and 3, we know noise perpendicular to the symmetry axis have non-negligible influence on the directional movement and diffusion.

$\langle V \rangle$ and D as functions of z axis noise intensity Q_z is reported in Fig.4. Unlike the effects of x axis and y axis noises, we find the average speed $|\langle V \rangle|$ has an obvious maximum with increasing Q_z ($\langle V \rangle < 0$ when $\Delta = -0.8$, and $\langle V \rangle > 0$ when $\Delta = 0.8$). So the generalized resonance transport phenomenon appears in the system. There exists

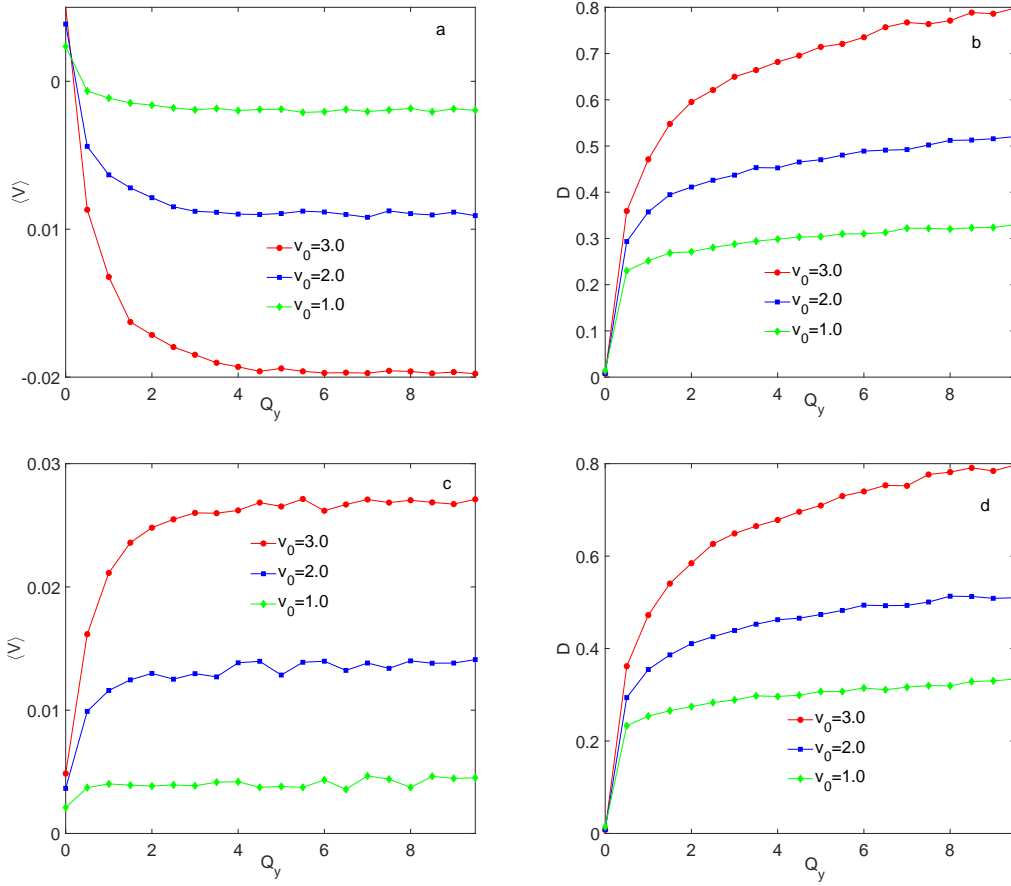


Figure 3. The average velocity $\langle V \rangle$ and diffusion coefficient D as functions of Q_y for different self-propelled speed v_0 . The other parameters are $L = 1.0$, $\varepsilon = 1.0$, $f = 1.8$, $Q_x = Q_z = 1.0$, $Q_\theta = Q_\varphi = 0.5$: (a) $\Delta = -0.8$, (b) $\Delta = -0.8$, (c) $\Delta = 0.8$, (d) $\Delta = 0.8$.

an optimum value of Q_z , and the current is very obvious at this point. Too large or too small Q_z will inhibit the directional movement speed. In Figs.4(b) and 4(d), we find the diffusion coefficient D monotonic decreases with increasing Q_z . So large Q_z will inhabit the diffusion. From Figs. 2, 3 and 4, we find an interesting phenomenon, that is the diffusion becomes obvious when the noise intensity perpendicular to the axis is large, but can be suppressed if the noise intensity parallel to the axis is large.

$\langle V \rangle$ and D as functions of polar angle noise intensity Q_θ is reported in Fig.5. We find whenever $\Delta = -0.8$ or $\Delta = 0.8$, $\langle V \rangle$ monotonic decreases with increasing Q_θ . In the case of $\Delta = -0.8$ (Fig.5(a)), the particle moves in $+z$ direction when $Q_\theta = 0.0$, and the direction changes from in $+z$ direction($\langle V \rangle > 0$) to in $-z$ direction($\langle V \rangle < 0$) with increasing Q_θ . So the current reverse phenomenon appears with increasing Q_θ . In the case of $\Delta = 0.8$, the particle moves always in $+z$ direction, and the speed becomes smaller and smaller with increasing Q_θ . Whenever $\Delta = -0.8$ or $\Delta = 0.8$, there exists an optimum value of Q_θ , and the diffusion is very obvious at this point(Fig.5(b) and Fig.5(d)).

The average velocity $\langle V \rangle$ and diffusion coefficient D as functions of the azimuth

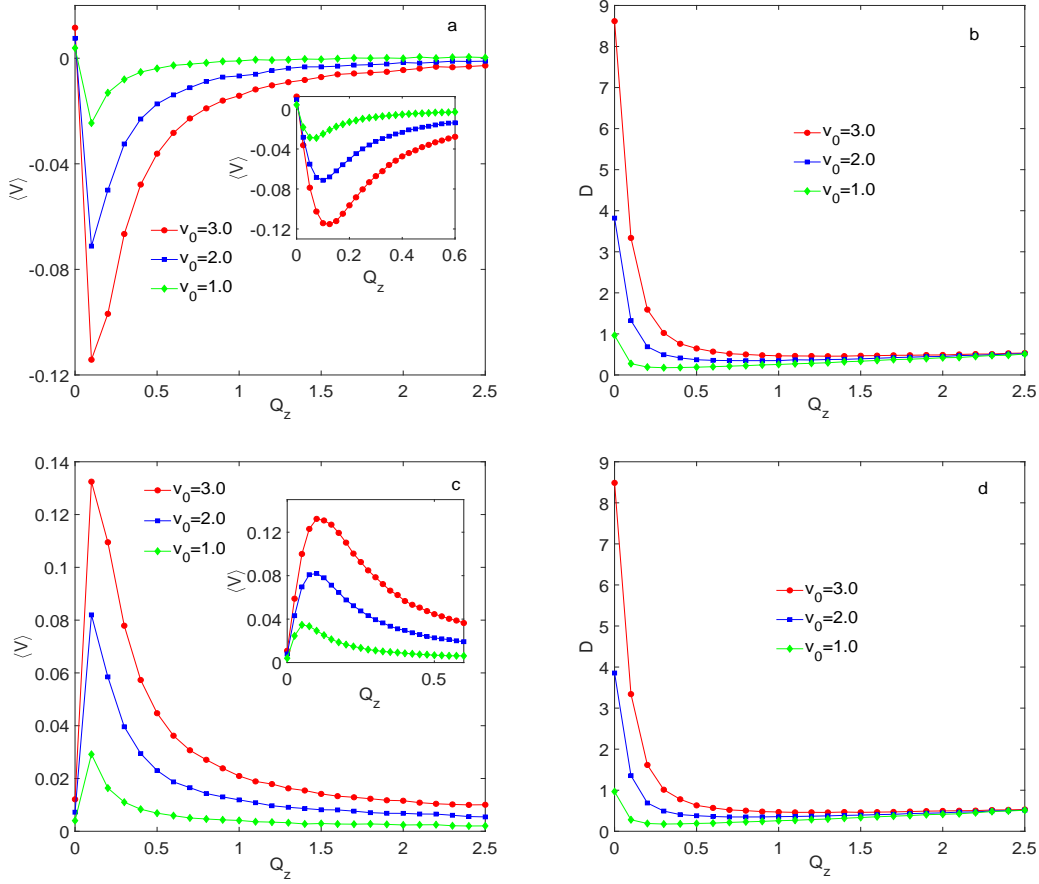


Figure 4. The average velocity $\langle V \rangle$ and diffusion coefficient D as functions of Q_z for different self-propelled speed v_0 . The other parameters are $L = 1.0$, $\varepsilon = 1.0$, $f = 1.8$, $Q_x = Q_y = 1.0$, $Q_\theta = Q_\varphi = 0.5$: (a) $\Delta = -0.8$, (b) $\Delta = -0.8$, (c) $\Delta = 0.8$, (d) $\Delta = 0.8$.

angle noise intensity Q_φ is reported in Fig.6. We find whenever $\Delta = -0.8$ or $\Delta = 0.8$, the average speed $|\langle V \rangle|$ and diffusion coefficient D increase with increasing noise intensity Q_φ . So large azimuth angle noise intensity will help to the current and the diffusion. $\langle V \rangle - Q_\varphi$ and $D - Q_\varphi$ curves change to horizon when Q_φ is large.

The average velocity $\langle V \rangle$ and diffusion coefficient D as functions of the channel parameter f with different v_0 is reported in Fig.7. We set $f \geq 1.0$ to avoid the channel becomes a enclosure space because the parameter ε is fixed ($\varepsilon = 1.0$). In Figs.7(a), we find $\langle V \rangle \rightarrow 0$ when $f = 1.0$, the reason is that the channel becomes a enclosure space and the particles are sealed in the enclosure space. $\langle V \rangle < 0$ and $\langle V \rangle$ has a minimum (The average speed $|\langle V \rangle|$ has a maximum) with increasing f . So there exits an optimal value of f that results in the most obvious current in $-z$ direction. In Fig.7(b), D monotonic increases with increasing f . So large f is good for the diffusion. In Fig.7(c), contrary to the result of Fig.7(a), we find $\langle V \rangle > 0$ and $\langle V \rangle$ has a maximum with increasing f . So there exits an optimal value of f that results in the maximum moving speed in z direction. Just like Fig.7(b), we find D monotonic increases with increasing f in Fig.7(d), so large f is good for diffusion. From the definition Eq.8 of the channel, we

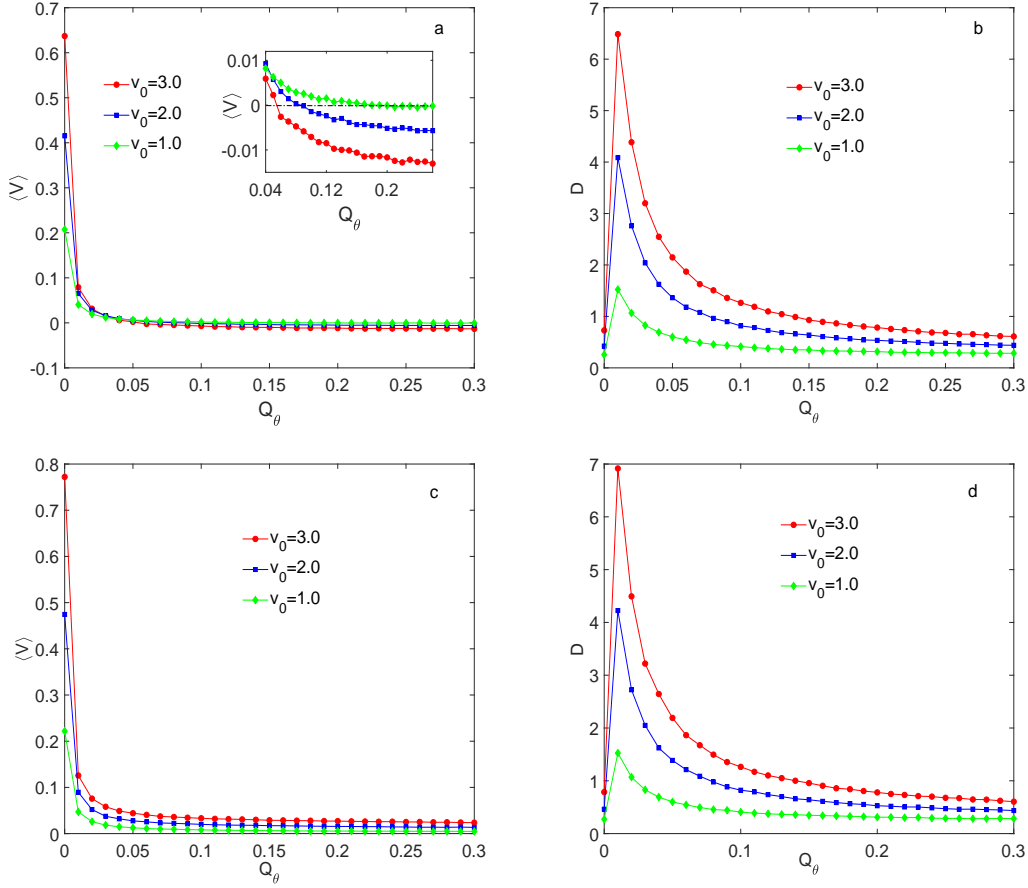


Figure 5. The average velocity $\langle V \rangle$ and diffusion coefficient D as functions of polar angle noise intensity Q_θ for different self-propelled speed v_0 . The other parameters are $L = 1.0$, $\varepsilon = 1.0$, $f = 1.8$, $Q_x = Q_y = Q_z = 1.0$, $Q_\varphi = 0.5$: (a) $\Delta = -0.8$, (b) $\Delta = -0.8$, (c) $\Delta = 0.8$, (d) $\Delta = 0.8$.

know the larger of f , the larger of the pore size is. In this case, too large pore size can not promote the directional moving speed but inhabit this phenomenon. However, large pore size is good for the diffusion of the particle.

The average velocity $\langle V \rangle$ and diffusion coefficient D as functions of the channel parameter ε with different v_0 is reported in Fig.8. In Fig.8(a), $\langle V \rangle$ has a maximum ($\langle V \rangle_{max} > 0$) and a minimum ($\langle V \rangle_{min} < 0$) with increasing ε . The $\langle V \rangle_{max}$ is on the left and the $\langle V \rangle_{min}$ is on the right. $\langle V \rangle \rightarrow 0$ when $|\varepsilon| > 1.8$ because channel will become a enclosure space. In Fig.8(b), D has a maximum with increasing ε ($\varepsilon = 0$). The channel changes to a straight tube when $\varepsilon = 0$, so straight tube is better for diffusion then corrugated pipe. In Fig.8(c), $\langle V \rangle$ has a minimum ($\langle V \rangle_{min} < 0$) and a maximum ($\langle V \rangle_{max} > 0$) with increasing ε . $\langle V \rangle_{min}$ is on the left and $\langle V \rangle_{max}$ is on the right. Just like Fig.8(a), $\langle V \rangle \rightarrow 0$ because the channel becomes a enclosure space when $|\varepsilon| > 1.8$. In this figure, we find the transport reverse phenomenon appears with increasing ε . In Fig.8(d), we find D has a maximum when the parameter $\varepsilon = 0$. That is, the diffusion is very obvious when the corrugated channel becomes a straight pipe.

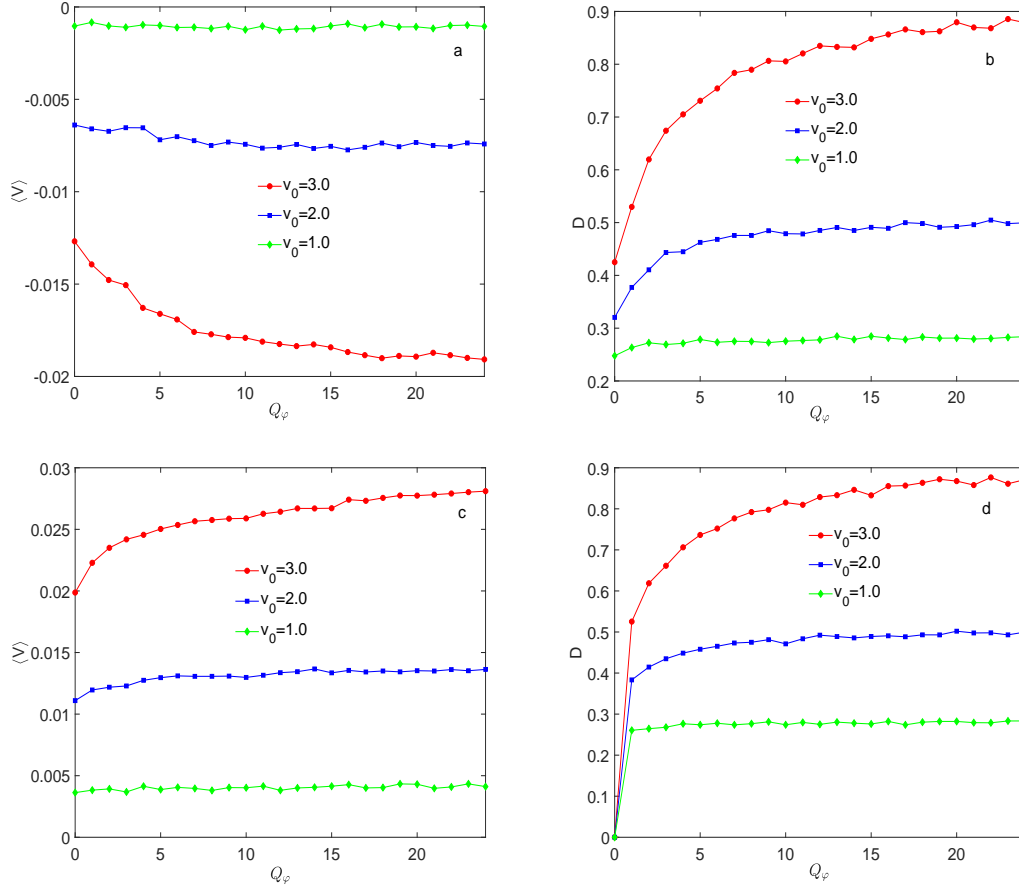


Figure 6. The average velocity $\langle V \rangle$ and diffusion coefficient D as functions of azimuth angle noise intensity Q_φ for different self-propelled speed v_0 . The other parameters are $L = 1.0$, $\varepsilon = 1.0$, $f = 1.8$, $Q_x = Q_y = Q_z = 1.0$, $Q_\theta = 0.5$: (a) $\Delta = -0.8$, (b) $\Delta = -0.8$, (c) $\Delta = 0.8$, (d) $\Delta = 0.8$.

The ratio $\langle V \rangle / v_0$ and diffusion coefficient D as functions of self-propelled speed v_0 with different adjust parameter Δ is reported in Fig.9. In Fig.9(a), the ratio $\langle V \rangle / v_0$ exists a minimum and a maximum with increasing v_0 . The particle moves in $-z$ direction when v_0 is small. The ratio $\langle V \rangle / v_0$ reaches a minimum first, then increases with increasing v_0 and reaches a maximum, then decreases with increasing v_0 again, and $\langle V \rangle / v_0 \rightarrow 0$ in the end. The current reverse phenomenon appears with increasing v_0 . In Fig.9(c), we find $\langle V \rangle > 0$ and $\langle V \rangle / v_0$ has a maximum with increasing self-speed v_0 . $\langle V \rangle / v_0 \rightarrow 0$ when v_0 is large. In Fig.9(b) and Fig.9(d), we find D has maximum with increasing v_0 , so proper value of v_0 is good for the diffusion, too small or too large v_0 will inhabit the diffusion.

The average velocity $\langle V \rangle$ and diffusion coefficient D as functions of the adjust parameter Δ is reported in Fig.10. In Fig.10(a), we find $\langle V \rangle$ first decreases with increasing Δ and reaches a minimum ($\langle V \rangle_{min} < 0$), then increases with increasing Δ and reaches a maximum ($\langle V \rangle_{max} > 0$), then decreases with increasing Δ in the end. There exist a minimum and a maximum in the $\langle V \rangle - \Delta$ curve, and the current reverse

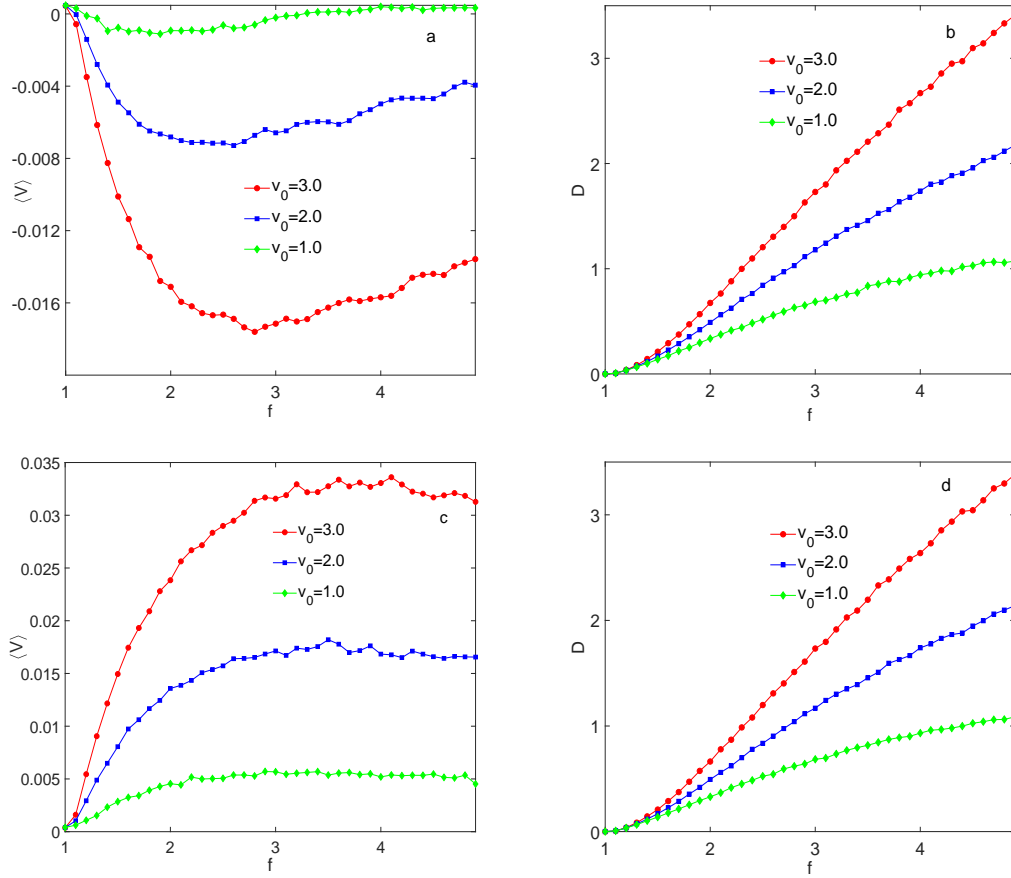


Figure 7. The average velocity $\langle V \rangle$ and diffusion coefficient D as functions of parameter f for different v_0 . The other parameters are $L = 1.0$, $\varepsilon = 1.0$, $Q_x = Q_y = Q_z = 1.0$, $Q_\theta = Q_\varphi = 0.5$: (a) $\Delta = -0.8$, (b) $\Delta = -0.8$, (c) $\Delta = 0.8$, (d) $\Delta = 0.8$.

phenomenon appears with increasing Δ . In Fig.10(b), we find the diffusion coefficient D reaches a maximum when the parameter $\Delta \rightarrow 0$.

3. Conclusions

In this paper, we numerically investigated the transport phenomenon of active particles confined in a 3D smooth channel with Gaussian noise. We find large noise intensity perpendicular to the symmetry axis is good for the current in the axis direction and the diffusion. The average speed has a maximum with increasing noise intensity parallel to the symmetry axis. The transport reverse phenomenon appears with increasing polar angle noise intensity when the adjust parameter Δ is negative. Large azimuth noise intensity is good for the current and diffusion. Changing the parameters ε and Δ can make different shape, and the transport reverse phenomenon appears with increasing ε and Δ . Proper size of pore is good for the directional current, but too large or too small pore size can inhabit this phenomenon. The diffusion is very obvious when the corrugated channel becomes a straight pipe.

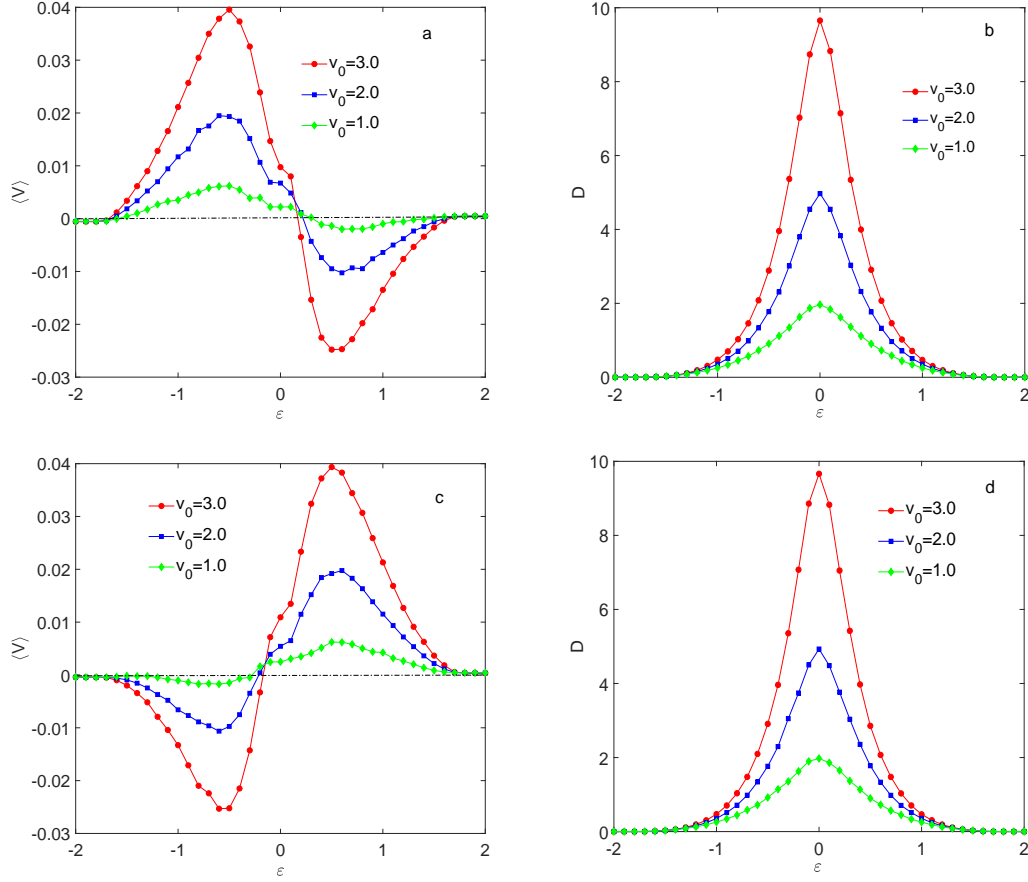


Figure 8. The average velocity $\langle V \rangle$ and diffusion coefficient D as functions of parameter ε for different v_0 . The other parameters are $L = 1.0$, $f = 1.8$, $Q_x = Q_y = Q_z = 1.0$, $Q_\theta = Q_\varphi = 0.5$: (a) $\Delta = -0.8$, (b) $\Delta = -0.8$, (c) $\Delta = 0.8$, (d) $\Delta = 0.8$.

4. Acknowledgments

Project supported by Natural Science Foundation of Anhui Province (Grant No:1408085QA11) and College Physics Teaching Team of Anhui Province (Grant No:2019jxtd046).

5. Referencing

- [1] S. Ramaswamy, 2010 *Annu. Rev. Condens. Matter Phys.* **1** 323.
- [2] M. C. Marchetti, J. F. Joanny, S. Ramaswamy, et al., 2013 *Rev. Mod. Phys.* **85** 1143.
- [3] D. Needleman, Z. Dogic, 2017 *Nat. Rev. Mater.* **2** 17048.
- [4] E. Pince, S. K. P. Velu, A. Callegari, et al., 2016 *Nat. Commun.* **7** 10907.
- [5] S. Palagi, P. Fischer, 2018 *Nat. Rev. Mater.* **3** 113.
- [6] P. Pietzonka, E. Fodor, C. Lohrmann, M. E. Cates, U. Seifert, 2019 *Phys. Rev. X* **9** 041032.
- [7] A. Kulkarni, S. P. Thampi, M. V. Panchagnula, 2019 *Phys. Rev. Lett.* **122** 048002.
- [8] J. C. Moreno, M. L. Rubio Puzzo, W. Paul, 2020 *Phys. Rev. E* **102** 022307.
- [9] G. Gompper, R. G. Winkler, T. Speck, A. Solon, C. Nardini, F. Peruani, et al., 2020 *J. Phys.: Condens. Matter* **32** 193001.

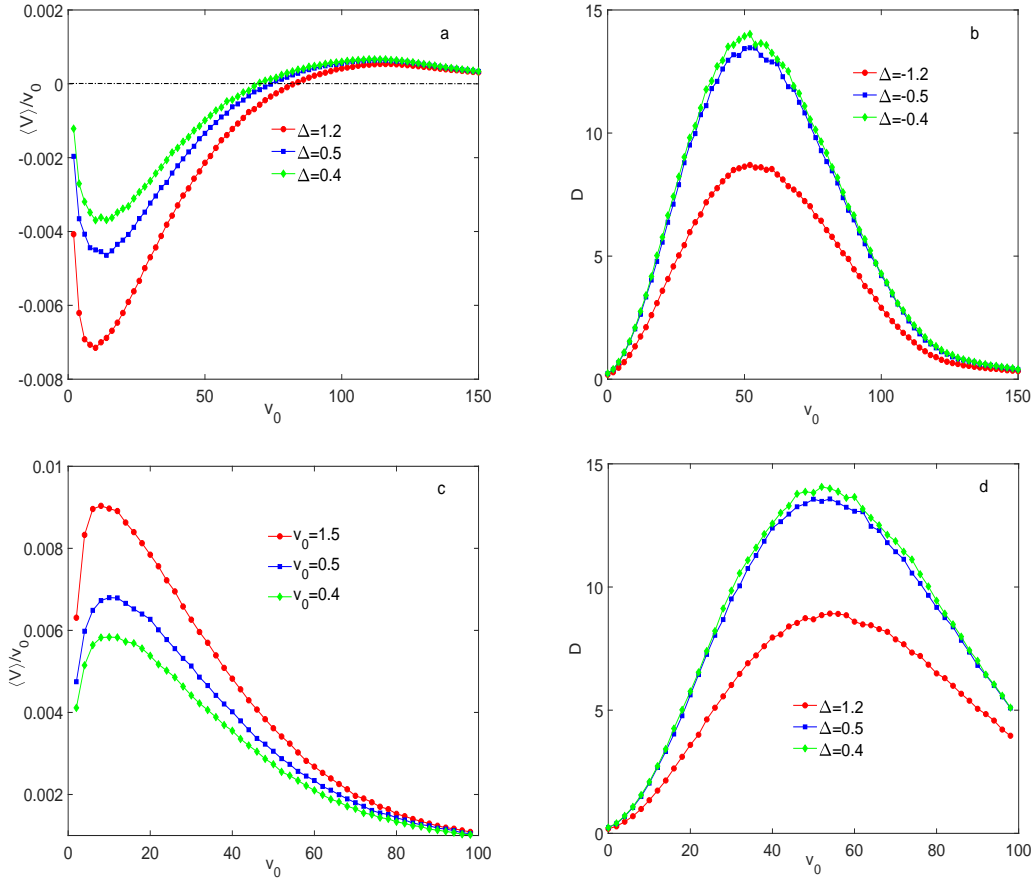


Figure 9. The ratio $\langle V \rangle / v_0$ and diffusion coefficient D as functions of v_0 for different Δ . The other parameters are $L = 1.0$, $\varepsilon = 1.0$, $f = 1.8$, $Q_x = Q_y = Q_z = 1.0$, $Q_\theta = Q_\varphi = 0.5$.

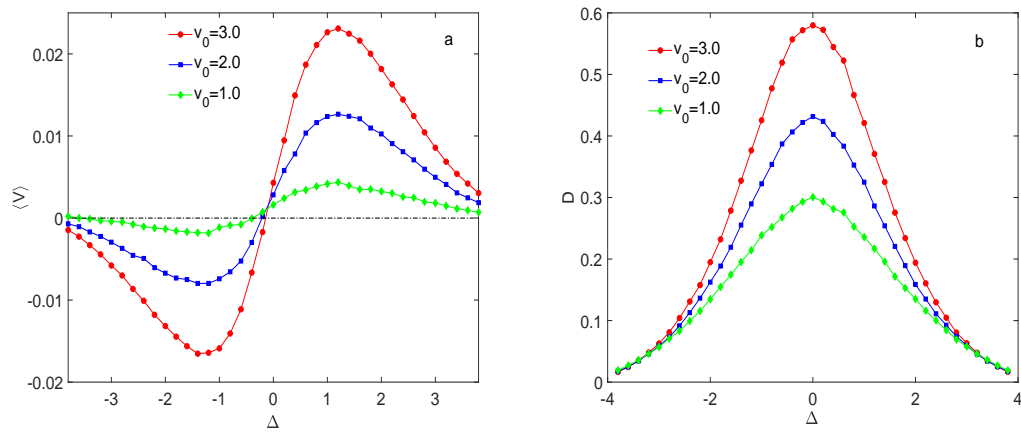


Figure 10. The average velocity $\langle V \rangle$ and the diffusion coefficient D as functions of adjust parameter Δ for different self-propelled speed v_0 . The other parameters are $L = 1.0$, $\varepsilon = 1.0$, $f = 1.8$, $Q_x = Q_y = Q_z = 1.0$, $Q_\theta = Q_\varphi = 0.5$.

- [10] S. Tang, F. Zhang, H. Gong, F. Wei, J. Zhuang, et al., 2020 *Sci. Robot.* **5** eaba6137.
- [11] H. X. Zhou, G. Rivas, A. P. Minton, 2008 *Annu. Rev. Biophys.* **37** 375.
- [12] B. Hille. Ion Channels of Excitable Membranes. Sinauer Associates, 3rd edition, 2001.ISBN 0878933212.
- [13] E. Beerdsen, D. Dubbeldam, B. Smit, 2005 *Phys. Rev. Lett.* **95** 164505.
- [14] E. Beerdsen, D. Dubbeldam, B. Smit, 2006 *Phys. Rev. Lett.* **96** 044501.
- [15] F. J. Keil, R. Krishna, M. O. Coppens, 2000 *Rev. Chem. Eng.* **16** 71.
- [16] T. M. Squires, S. R. Quake, 2005 *Rev. Mod. Phys.* **77** 977.
- [17] D. Pedone, M. Langecker, G. Abstreiter, U. Rant. 2011 *Nano Lett.* **11** 1561.
- [18] Z. Siwy, I. D. Kosinska, A. Fulinski, C. R. Martin, 2005 *Phys. Rev. Lett.* **94** 048102.
- [19] C. Hu, Y. Ou, J. Wu, Q. Chen, B. Ai, 2015 *J. Stat. Mech.* **2015** 05025.
- [20] H. W. Hu, L. Du, L. H. Qu, Z. L. Cao, Z. C. Deng , Y. C. Lai, 2021 *Phys. Rev. Research* **3** 033162.
- [21] B. Wang, H. Chen, Y. Wu, 2020 *Physica A* **537** 122779.
- [22] J. Richardi, M. P. Pileni, J. J. Weis, 2009 *J. Chem. Phys.* **130** 124515.
- [23] C. Iss, D. Midou, A. Moreau, D. Held, et al., 2019 *Soft Matter* **15** 2971.
- [24] P. K. Ghosh, V. R. Misko, F. Marchesoni, F. Nori, 2013 *Phys. Rev. Lett.* **110** 268301.
- [25] X. Ao, P. K. Ghosh, Y. Li, G. Schmid, P. Hänggi, F. Marchesoni, 2015 *EPL* **109** 10003.
- [26] C. Bechinger, R. Di Leonardo, H. Löwen, C. Reichhardt, G. Volpe, G. Volpe, 2016 *Rev. Mod. Phys.* **88** 045006.
- [27] A. Murali, P. Dolai, A. Krishna, K. Vijay Kumar, S. Thutupalli, 2022 *Phys. Rev. Research* **4** 013136.
- [28] Z. Liu, L. Du , W. Guo , D. Mei, 2016 *Eur. Phys. J. B* **89** 222.
- [29] F. Li, B. Ai, 2017 *Physica A* **484** 27.
- [30] A. Pototsky, U. Thiele, H. Stark, 2016 *Eur. Phys. J. E* **39** 51.
- [31] P. Hänggi, F. Marchesoni, S. Savelev, G. Schmid, 2010 *Phys. Rev. E* **82** 041121.
- [32] Y. Han, A. M. Alsayed, M. Nobili, J. Zhang, T. C. Lubensky, A. G. Yodh, 2006 *Science* **314** 626.
- [33] M. Pu, H. Jiang, Z. Hou, 2017 *Soft Matter* **13** 4112.
- [34] Y. He, B. Ai, 2010 *Phys. Rev. E* **81** 021110.
- [35] L. Machura, M. Kostur, P. Talkner, J. Luczka, F. Marchesoni, P. Hänggi, 2004 *Phys. Rev. E* **70** 061105.
- [36] P. Reimann, C. Van den Broeck, H. Linke, P. Hänggi, J. M. Rubi, A. Perez-Madrid, 2001 *Phys. Rev. Lett.* **87** 010602.